

Relationship of Prefrontal Connections to Inhibitory Systems in Superior Temporal Areas in the Rhesus Monkey

H. Barbas^{1,2,3,4}, M. Medalla¹, O. Alade¹, J. Suski¹,
B. Zikopoulos¹ and P. Lera¹

¹Department of Health Sciences, Boston University, Boston, MA, USA, ²Program in Neuroscience, Boston University, Boston, MA, USA, ³NEPRC, Harvard Medical School, Boston, MA, USA and ⁴Department of Anatomy and Neurobiology, Boston University School of Medicine, Boston, MA, USA

The prefrontal cortex selects relevant signals and suppresses irrelevant signals in behavior, as exemplified by its functional interaction with superior temporal cortices. We addressed the structural basis of this process by investigating quantitatively the relationship of prefrontal pathways to inhibitory interneurons in superior temporal cortices. Pathways were labeled with neural tracers, and two neurochemical classes of inhibitory interneurons were labeled with parvalbumin (PV) and calbindin (CB), which differ in mode of inhibitory control. Both markers varied significantly and systematically across superior temporal areas. Calbindin neurons were more prevalent than PV neurons, with the highest densities found in posterior high-order auditory association cortices. Axons from anterior lateral, medial prefrontal and orbitofrontal areas terminated in the anterior half of the superior temporal gyrus, targeting mostly the superficial layers (I to upper III), where CB neurons predominated. Reciprocal projection neurons were intermingled with PV neurons, and emanated mostly from the deep part of layer III and to a lesser extent from layers V–VI, in proportions matching the laminar density of inhibitory interneurons. In marked contrast, prefrontal connections in temporal polar cortex were found mostly in the deep layers, showing mismatch with the predominant upper laminar distribution of interneurons. Differences in the relationship of connections to inhibitory neurons probably affect the dynamics in distinct superior temporal cortices. These findings may help explain the reduced efficacy of inhibitory control in superior temporal areas after prefrontal cortical damage.

Keywords: auditory association areas, calbindin neurons, dorsolateral prefrontal cortex, medial prefrontal cortex, parvalbumin neurons, prefrontal inhibitory control

Introduction

The prefrontal cortex exercises executive control by selective attention to behaviorally relevant information and inhibition of irrelevant information (for reviews see Fuster, 1989; Roberts and Wallis, 2000; Miller and Cohen, 2001). While once it was thought that inhibitory control was uniquely dependent on orbitofrontal and ventrolateral prefrontal cortices, there is now evidence in both human and non-human primates that all prefrontal cortices have a role in inhibitory control, albeit within the domain of their specialization (for reviews see Shimamura, 1995; Roberts and Wallis, 2000).

The phenomenon of inhibitory control is exemplified at the functional level in the interaction of prefrontal cortex with superior temporal auditory association cortices. Humans with dorsolateral prefrontal lesions are impaired when irrelevant auditory stimuli are introduced in an auditory discrimination task. Moreover, their performance is highly correlated with decreased activity in dorsolateral prefrontal cortices and a con-

comitant increase of activity in auditory association cortices (Chao and Knight, 1998). Similar behavioral/neurophysiological correlates have been reported for aged humans, suggesting that neural changes in prefrontal cortices reduce inhibitory influences in auditory areas, and impair the ability to ignore irrelevant sounds (Chao and Knight, 1997).

There is also a close functional association between medial prefrontal and temporal auditory association areas. Electrical stimulation of the cingulate vocalization cortices (areas 32, 24, 25) decreases auditory evoked activity in superior temporal auditory cortices (Müller-Preuss *et al.*, 1980; Müller-Preuss and Ploog, 1981). Parallel evidence from imaging studies in humans indicates that cognitive tasks involving verbal fluency activate the anterior cingulate region and reduce activity in superior temporal auditory cortices (Dolan *et al.*, 1995; Frith and Dolan, 1996).

Evidence that the prefrontal cortex can select relevant auditory signals and ignore irrelevant signals emerged from behavioral studies, but the structural basis of this functional interaction remains obscure. One way that neural interaction between these linked areas may be gated is through termination of prefrontal axons within a superior temporal microenvironment populated by distinct classes of inhibitory interneurons. In addition, neurons in auditory association cortices that project to prefrontal cortices may be influenced by local inhibitory neurons.

Previous studies have demonstrated the existence of pathways linking prefrontal cortices with superior temporal areas (e.g. Jacobson and Trojanowski, 1977; Müller-Preuss *et al.*, 1980; Barbas and Mesulam, 1985; Vogt and Pandya, 1987; Petrides and Pandya, 1988; Barbas, 1988; Hackett *et al.*, 1999; Romanski *et al.*, 1999b; Kondo *et al.*, 2003). However, the relationship of prefrontal connections to local inhibitory neurons in the superior temporal cortex is not known. The present study addressed this issue by focusing on the laminar relationship of prefrontal connections to two distinct neurochemical classes of inhibitory neurons in superior temporal cortices identified by the calcium-binding proteins parvalbumin (PV) and calbindin (CB) (Hendry *et al.*, 1989). The choice of these two markers is based on several factors. First, PV positive neurons are found preferentially in the middle layers of the cortex (e.g. Hendry *et al.*, 1989; DeFelipe *et al.*, 1989b), which receive 'forward' type projections. In contrast, CB-positive neurons are found predominantly in the upper layers of the cortex (e.g. Hendry *et al.*, 1989; DeFelipe *et al.*, 1989a, 1990; Peters and Sethares, 1997), the chief targets of corticocortical 'feedback' projections. Second, the two neurochemical classes of inhibitory interneurons differ in their site of innervation of other neurons. Parvalbumin is expressed in basket and chandelier cells, which

innervate pyramidal cell bodies, proximal dendrites and axon initial segments (DeFelipe *et al.*, 1989b; Kawaguchi and Kubota, 1997; Shao and Burkhalter, 1999). On the other hand, CB is expressed in inhibitory double bouquet cells in the cortex, which innervate distal dendrites and spines of other neurons (e.g. DeFelipe *et al.*, 1989a; Peters and Sethares, 1997). In addition, we previously found that the two classes of neurochemically identified inhibitory interneurons show systematic quantitative differences in their regional distribution in the prefrontal cortices (Dombrowski *et al.*, 2001), which are connected with superior temporal cortices (for review see Barbas, 1992). Regional variations in distinct types of interneurons have also been noted in some sensory and other association cortices in primates (e.g. Kritzer *et al.*, 1992; Kondo *et al.*, 1994; Mikkonen *et al.*, 1997; DeFelipe *et al.*, 1999; Kondo *et al.*, 1999; Elston and Gonzalez-Albo, 2003).

Here we first investigated whether the two classes of neurochemically identified inhibitory interneurons show differences in their regional and laminar distribution in superior temporal cortices. We then investigated the laminar relationship of prefrontal connections to inhibitory neurons in superior temporal areas. Our analysis of connections was restricted to medial areas 32 and 9, rostral lateral areas 10 and 9, and several orbitofrontal areas, all of which are connected with the anterior half of the superior temporal gyrus (Barbas and Mesulam, 1985; Barbas, 1993; Carmichael and Price, 1995; Barbas *et al.*, 1999). We provide evidence that prefrontal connections are found in distinct laminar microenvironments in different superior temporal cortices, in patterns that likely affect the local excitatory and inhibitory dynamics.

Materials and Methods

Surgical Procedures

Experiments were conducted on adult rhesus monkeys (*Macaca mulatta*). The monkeys were anesthetized with ketamine hydrochloride (10–15 mg/kg, i.m.) followed by isoflurane until a surgical level of anesthesia was accomplished. The monkeys were then placed in a stereotaxic apparatus and a small region of the cortex was exposed. Surgery was performed under aseptic conditions while heart rate, muscle tone, respiration and pupillary dilatation were closely monitored.

Injection of Neural Tracers

Injections of the anterograde tracer biotinylated dextran amine (BDA, Molecular Probes, Eugene, OR; 10 mg/ml; 3–10 μ l) were placed in five rhesus monkeys using a microsyringe (Hamilton, Reno, NV, CAT#80383) mounted on a microdrive. BDA is an excellent anterograde tracer that labels the entire extent of axonal terminals and boutons. In all cases, 2–4 penetrations were made and BDA was injected 1.2–1.6 mm below the pial surface.

Injections of retrograde tracers were placed in nine rhesus monkeys in medial and dorsal prefrontal areas (areas 32, 9 and 10), and in orbitofrontal areas (areas OPro, OPAl/OPro, 13 and 11). The tracers used included horseradish peroxidase-wheatgerm agglutinin (HRP-WGA; five cases; total volume 0.1 μ l), and the fluorescent tracers fast blue (two cases, total volume 0.4 μ l), and diaminidino yellow (one case, total volume 0.4 μ l). In each case the tracer was injected in two penetrations separated by ~0.5 mm at a depth of 1.2–1.6 mm below the pial surface. A period of 10–15 min was allowed for each injection for adequate dye penetration at the injection site.

Perfusion and Tissue Processing

In cases with injection of BDA the survival period was 18 days. The animals were then anesthetized with a lethal dose of sodium pentobarbital (>50 mg/kg, to effect) and perfused with 4% paraformaldehyde, or 4% paraformaldehyde and 0.2% glutaraldehyde in 0.1 M phosphate

buffer (pH 7.4). The brain was removed from the skull, photographed and cryoprotected in graded solutions of sucrose (10–30% in 0.1 M PBS). In cases with injection of HRP-WGA the survival period was 2 days, and in cases with fluorescent dye injections the survival period was 10 days (two cases), or 18 days when there was a BDA injection in the opposite hemisphere in the same case (two cases). All brains were frozen in -75°C isopentane (Fisher, CAT#03551-4) and cut on a freezing microtome in the coronal plane at 40 or 50 μ m in 10 series. Perfusion, cryoprotection and the histochemical assay in HRP-WGA cases were according to previous studies (Dermon and Barbas, 1994). In cases with injection of fluorescent tracers, projection neurons were viewed from one series of sections mounted directly on glass slides after cutting.

Immunocytochemical Procedures

PV and CB (Brightfield)

To investigate the distribution of neurons positive for parvalbumin or calbindin in superior temporal cortex using unbiased stereological methods, we performed immunocytochemical procedures in one series of sections for each marker. Sections from one series were processed simultaneously under uniform conditions. The tissue was washed with 0.1 M PBS (pH 7.4) and preblocked with 10% normal goat serum (with 0.2% Triton-X) for 1 h, and incubated for 2–3 days in primary antibody for PV (1:2000; mouse monoclonal, Chemicon), or CB (1:2000; mouse monoclonal, Accurate Chemical and Scientific Corp.). The tissue was then placed for 3 h in biotinylated goat-anti-mouse IgG (1:200; Vector Laboratories), followed by 1 h incubation in avidin-biotin complex (Vector Laboratories). The tissue was then processed using diaminobenzidine tetrahydrochloride (DAB kit, Zymed) and rinsed in PB.

PV and CB (Immunofluorescence)

To investigate the relationship of prefrontal connections to neurons positive for parvalbumin (PV+) or calbindin (CB+) in superior temporal areas directly, we performed immunocytochemical procedures in series of sections that contained fluorescent labeled projection neurons directed to prefrontal cortices. Tissue sections from each series were washed with 0.1 M PBS (pH 7.4) and preblocked with 10% goat serum (with 0.2% Triton-X) for 1 h, and incubated for 2–3 days in primary antibody for PV (1:2000; mouse monoclonal, Chemicon), or CB (1:2000; mouse monoclonal, Accurate Chemical and Scientific Corp.). The tissue was then placed overnight in goat-anti-mouse IgG (for CB or PV) conjugated with the fluorescent probe Cyanoindocarbocyanine (Cy3, Chemicon, 1:800), or Alexa 488 (Molecular Probes, 1:100; with 0.1% Triton-X and 1% normal goat serum) and rinsed in PB.

BDA (Brightfield)

To visualize labeled boutons in superior temporal cortices we processed two adjacent series of sections using immunocytochemical procedures. Sections from each series were washed in 0.1 M PBS and placed overnight in avidin-biotin HRP complex (Vector Laboratories; diluted 1:100 in 0.1 M PBS with 0.2 Triton X). The sections were then washed and processed for immunoperoxidase reaction using DAB (Zymed). One series of sections was mounted, dried and every other section stained for Nissl for mapping at the light microscope.

Double Immunocytochemistry (Brightfield)

To visualize labeled boutons and CB+ or PV+ neurons simultaneously using brightfield microscopy, we first processed tissue for BDA (as described above) and then placed it in primary antibody for CB or PV, followed by a secondary antibody (as above). The tissue was then incubated in the A and B solution (Vectastain PK 4000 Avidin-Biotin Peroxidase Kit, Vector Laboratories) with Triton-X, washed in PBS and incubated in VIP (Vector Laboratories) for ~10 s. The BDA reaction product (brown) was clearly distinguishable from the VIP reaction product (purple).

Data Analysis

Stereological Analysis

To estimate the density of PV+ and CB+ neurons in temporal cortices in three dimensions we performed stereological procedures (for a review

see Howard and Reed, 1998) using a semi-automated commercial system (StereoInvestigator, Microbrightfield, Colchester, VT). Boundaries of areas were placed from coronal tissue sections with PV+ and CB+ neurons counterstained for Nissl, based on the architectonic map of Galaburda and Pandya (1983). Separate counts were made for the superficial (layers I-III) and deep layers (IV-VI).

We considered several parameters in estimating the density of each neurochemical class of neurons, including the coefficient of error (CE) (which was set to <10%), target cell counts, section interval, counting frame size, grid size, section thickness and guard zone size (West and Gundersen, 1990; West *et al.*, 1991; Gundersen *et al.*, 1999). Section thickness was adequate for using the optical disector, where counting is restricted to a fraction of the tissue thickness, and includes a guard zone to avoid error due to cell plucking or cell splitting during tissue sectioning. Section thickness was 50 μm after cutting, which shrank to 15 μm after mounting on gelatin-coated slides. The guard zone was set at 2 μm for the top and bottom of the tissue section, leaving 11 μm in the counting brick zone. After pilot study, the frame was set at 150 \times 150 μm .

Density Estimate of CB+ and PV+ Neurons in Two Dimensions

We also estimated the density of CB+ and PV+ neurons in another three animals in tissue processed for immunofluorescence, using exhaustive counting of labeled neuronal profiles in two dimensions. This practical method (for discussion see Benes and Lange, 2001) made it possible to visualize and map simultaneously neurochemical markers of interneurons as well as projection neurons in some of the cases with injection of fluorescent tracers. Mapping was accomplished by viewing brain sections with a fluorescence microscope (Nikon, Optiphot), equipped with an encoded stage and coupled electronically to a PC computer. This system makes it possible to map labeled neurons in precise register with anatomical landmarks and to count them within each area of interest. Software developed in our laboratory ensured that each labeled neuron was counted only once, as described previously (Barbas and De Olmos, 1990).

Maps of Labeled Projection Neurons in Superior Temporal Areas

After injection of fluorescent tracers in prefrontal cortices, we used one series of sections to conduct systematic exhaustive mapping of labeled projection neurons on the ipsilateral side in superior temporal cortices (1 in every 10 sections). We viewed brain sections with a fluorescence microscope (Nikon, Optiphot), equipped with an encoded stage and coupled electronically to a PC computer, as described above. In some cases we plotted labeled neurons using a commercial system (NeuroLucida, Microbrightfield), coupled to a microscope (Olympus, BX60). After plotting, sections were counterstained with thionin and returned to the microscope to delineate layers, count labeled neurons and measure the area occupied by each layer in individual temporal areas. We used the same systems to map labeled neurons in cases with injection of HRP-WGA using brightfield illumination.

Normalized Density of Projection Neurons, CB+ and PV+ Neurons in Superior Temporal Areas

We normalized the data to determine the relative density of projection neurons in each superior temporal area, by expressing the number of labeled projection neurons in each superior temporal area as a percentage of the total number in all superior temporal areas in each case. We also estimated the density of fluorescent labeled PV+ or CB+ neurons by dividing the total number of labeled neurons in two laminar compartments (layers I-III and IV-VI) by the volume of the tissue examined in each compartment for each area, expressed as neurons per mm^2 . This made it possible to determine the relationship of the density of connections in superior temporal areas to the density of PV+ or CB+ neurons in each area.

Maps of Labeled Axonal Terminations in Superior Temporal Areas

To outline and map labeled boutons in the superior temporal cortices we used brightfield illumination and a semi-automated system (NeuroLucida). We examined all sections in one series (representing 1 in 10 sections through the superior temporal region), identified architectonic areas within each section, and conducted exhaustive mapping of

boutons quantitatively by area and layer. We obtained relative density data by expressing the number of labeled boutons in each area as a percentage of the total in superior temporal areas in that case. We then normalized the data for each area to determine the percentage found in the superficial (layers I-III) and deep (IV-VI) layers.

Anterograde labeling after injection of HRP-WGA does not appear as discrete boutons as seen with BDA label. In the single case with HRP-WGA for anterograde analysis (case AM) we obtained the optical density of anterograde labeling using an image analysis system (MetaMorph, Universal Imaging System Corp., West Chester, PA), as described previously (Rempel-Clower and Barbas, 2000). This system uses a CCD camera (Dage-MTI, Michigan City, IN) mounted on the microscope to capture images directly from brain sections. Measurements of anterograde label were made under darkfield illumination using a fiber optic illuminator (Optical Analysis Corp., Nashua, NH) at a magnification of 100 \times . To determine the laminar pattern of anterograde label, data were normalized so that the density in the upper layers (mean density in layers I-III) and the lower layers (mean density in layers IV-VI) was expressed as a percentage of the total in that area. In previous studies, this quantitative method has provided the same results as qualitative analyses (Barbas and Rempel-Clower, 1997; Rempel-Clower and Barbas, 1998; Barbas *et al.*, 1999).

Comparison of Connections to Inhibitory Interneurons

Comparisons were made for normalized data for the density of inhibitory neurons and connections. For this comparison we included areas with significant label (>20 neurons or >50 boutons). For optical density analysis the lower limit was equivalent to the level detectable above background, measured using an imaging analysis system (MetaMorph, Universal Imaging), as described above. Background level was obtained by an initial density measure in each section in an area with no anterograde label, which was subtracted from subsequent measures. Using this method, the lightest label is up to 17% of the densest label (Rempel-Clower and Barbas, 2000), and corresponds to ~50 boutons in cases with BDA label. Boutons labeled with BDA can be counted unambiguously as single entities. The lower limit for projection neurons is based on our experience that 20 labeled neurons/area show a comparable laminar distribution as denser long-distance corticocortical projections. In the cases studied <20 neurons represent 1-13% of the densest label.

Photography

High-resolution photomicrographs of labeled boutons, varicose fibers or neurons in superior temporal areas were captured with a CCD camera on an Olympus BX51 microscope connected to a PC using a commercial imaging system (MetaMorph v.4.1, Universal Imaging Corp.). Image stacks of several focal planes were acquired in each area of interest resulting in pictures of 50 μm thick sections focused throughout their z-axis extent. This procedure was used to capture images at high depth of field of BDA-labeled boutons or projection neurons, as well as PV+ or CB+ neurons in superior temporal areas labeled with different fluorescent probes and tracers. Stacked images from adjacent serial sections were superimposed to highlight the differential distribution of labeled neurons. Figures were prepared with Adobe Photoshop (Adobe Systems Inc., San Jose, CA) and overall brightness and contrast were adjusted without retouching.

Superior Temporal Nomenclature

The nomenclature for superior temporal cortices is varied in the literature, though there is considerable agreement on the borders of many of its subdivisions. A detailed comparison of the nomenclature across studies for auditory-related areas is included in the maps of Hackett *et al.* (1998), and in our previous study (Barbas *et al.*, 1999). Below we include a brief review of the nomenclature found in the literature; the list is not exhaustive.

The architectonic study of Galaburda and Pandya (1983) includes the entire superior temporal region. The most rostral extent of the superior temporal cortex includes dysgranular and agranular areas in the dorsal and dorsomedial parts of the temporal pole. This polar region was labeled area Pro (Galaburda and Pandya, 1983) and corresponds to area 38 of Brodmann (1909), area TG (Von Bonin and Bailey, 1947), TPa-p

and TPdg (Mesulam and Mufson, 1982), areas TPpAll and TPproD (Gower, 1989), and dorsal area 36 (Suzuki and Amaral, 1994, 2003). In this study, we have used the descriptive terminology dorsomedial (DM) and dorsal pole (DP) for this region. Immediately caudal to the temporal pole are areas Ts1 and Ts2 (Galaburda and Pandya, 1983). The temporal pole, area Ts1 and most of Ts2 are situated anterior to auditory association areas mapped in physiologic studies (for discussion see Hackett *et al.*, 1998). However, a recent functional mapping study has demonstrated that the entire superior temporal gyrus, including the temporal pole, and the superficial part of the upper bank of the superior temporal sulcus are responsive to auditory stimuli (Poremba *et al.*, 2003), and the temporal pole is responsive to species-specific vocalizations (Poremba *et al.*, 2004). However, in addition to processing auditory stimuli, these areas may have polymodal features like the adjoining cortex in the superior temporal sulcus (for review see Cusick, 1997).

Most other studies in the literature have focused on auditory-related areas of the superior temporal gyrus, which were mapped using classic physiological and connectional procedures, as well as recently introduced chemoarchitectonic methods (Morel *et al.*, 1993; Molinari *et al.*, 1995; Jones *et al.*, 1995; Kosaki *et al.*, 1997; Hackett *et al.*, 1998; Tian *et al.*, 2001; reviewed in Kaas and Hackett, 2000). The following areas described in Galaburda and Pandya (1983) correspond to areas mapped physiologically (see Hackett *et al.*, 1998), as shown in parentheses: area Ts3 (RP and RTL), area paI (RTM), area proA (RM), area paAr (RT), reIt (CM), paAlt (AL and part of RP), paAc (CL and posterior part of A1), Tpt (CP and Tpt), KA (A1 and R). Area paI and proA appear to overlap with area M of Kosaki *et al.* (1997). The primary auditory area (A1) and area R are largely coextensive in the maps of Merzenich and Brugge (1973), Jones *et al.* (1995) and Hackett *et al.* (1998).

The nomenclature used here is based largely on the architectonic study of Galaburda and Pandya (1983), which includes the entire superior temporal region, with references to other maps, where possible.

Results

Distribution of Two Distinct Classes of Neurons Positive for CB or PV in Superior Temporal Areas

We mapped the pattern of distribution of PV+ and CB+ neurons from three animals and estimated their density using a two-dimensional (2D) approach in tissue immunostained with fluorescent probes. Calbindin positive neurons were found in all layers, but they were most prevalent in a band in the superficial layers, particularly layer II. On the other hand, PV+ neurons were most densely distributed in a central band at the bottom of layer III, layer IV and upper part of layer V (Fig. 1A–C). These findings are consistent with the complementary laminar distribution of these neurochemical classes of neurons (Hendry *et al.*, 1989; DeFelipe *et al.*, 1989a, 1990).

We obtained quantitative stereological data on the 3D distribution and density of CB+ and PV+ neurons in another three animals, using tissue processed with DAB for brightfield microscopy. Neurons positive for CB or PV were widely distributed in superior temporal areas with some regional variation, as shown in Figure 2. In all areas CB+ neurons outnumbered the parvalbumin, but to a different extent. The two neuronal populations were comparable in areas Ts1–Ts3. However, in the temporal pole, the primary auditory area (KA, or A1) or its neighbors (areas proA, paAlt), and particularly in posterior superior temporal areas (areas reIt, paAc and Tpt), CB+ neurons outnumbered the parvalbumin by 50–100% (ANOVA, $P = 0.0002$).

There were overall differences in the distribution of CB+ neurons in superior temporal cortices ($P = 0.03$). The density of CB+ neurons was higher in the superficial layers (I–III) than in

the deep layers (IV–VI) in all areas, but showed regional variation (Fig. 3). The superficial and deep neuronal distributions were comparable in the dorsomedial and dorsal part of the temporal pole (DM/DP). In contrast, CB+ neurons were more densely distributed in the upper layers in the primary auditory area (KA or A1) and neighboring areas (areas paAlt and proA) and in caudal superior temporal areas (areas reIt, paAc, and Tpt). There were marked areal differences in the density of CB+ in the superficial layers among superior temporal areas ($P = 0.001$), but not in the deep layers (Fig. 3).

There were small but consistent differences in PV+ neurons among superior temporal areas (Fig. 2A). Parvalbumin-positive neurons were least prevalent in rostral (temporal pole), or caudal (areas reIt, paAc) superior temporal areas, a pattern that is consistent with findings in humans (Chiry *et al.*, 2003). In contrast to the distribution of CB+ neurons, PV+ neurons were more prevalent in the deep layers (IV–VI) than in the superficial (I–III) in most areas (Fig. 4). An exception to this pattern was noted in the dorsomedial and dorsal parts of the temporal pole rostrally (DM/DP), and areas proA, paAc and Tpt caudally, where the distributions in the upper layers were either slightly higher, or comparable to the deep layers (Fig. 4). There were overall differences in the regional density of PV+ neurons ($P = 0.003$), which could be attributed to regional differences in the deep layers (IV–VI, $P = 0.0004$). In contrast, there was no significant difference in the distribution of PV+ neurons in the superficial layers ($P > 0.05$), showing a laminar pattern that was the opposite of CB.

When the entire distribution of CB+ and PV+ neurons was considered together, there was no significant regional variation, consistent with the complementary pattern of these two markers of neurochemically identified inhibitory interneurons (Fig. 5A). However, the overall density of CB+ and PV+ neurons in the superficial (I–III) in comparison with the deep layers (IV–VI) differed significantly, due to a higher density of the two markers in the superficial layers (t -test = 6.86, $P = 0.0004$), but not in the deep layers. Moreover, among superior temporal areas the density of the combined CB+ and PV+ neurons differed significantly in layers I–III ($P = 0.004$), but not for layers IV–VI (Fig. 5B). A very similar overall distribution of CB+ and PV+ neurons was seen when their normalized density was calculated in two dimensions in tissue processed for immunofluorescence (Fig. 5C). Tissue used for the 2D estimate of CB+ and PV+ neurons also contained projection neurons or labeled fibers in some cases, in order to visualize the relationship of these populations directly (Fig. 1D–I).

Prefrontal Connections in Superior Temporal Cortices

Injection Sites

The injection sites in all cases are shown on the medial (Fig. 6A), lateral (Fig. 6B) and basal (Fig. 6C) surfaces. The areas chosen for study have robust and common connections primarily with the anterior half of the superior temporal gyrus (Barbas *et al.*, 1999). The study does not include the connections of dorsal area 8 or caudal area 46, which are connected with posterior superior temporal cortices, and probably have a different functional relationship with auditory association areas (e.g. Barbas and Mesulam, 1981, 1985; Petrides and Pandya, 1988; Barbas, 1988; Romanski *et al.*, 1999a,b; for review see Pandya *et al.*, 1988).

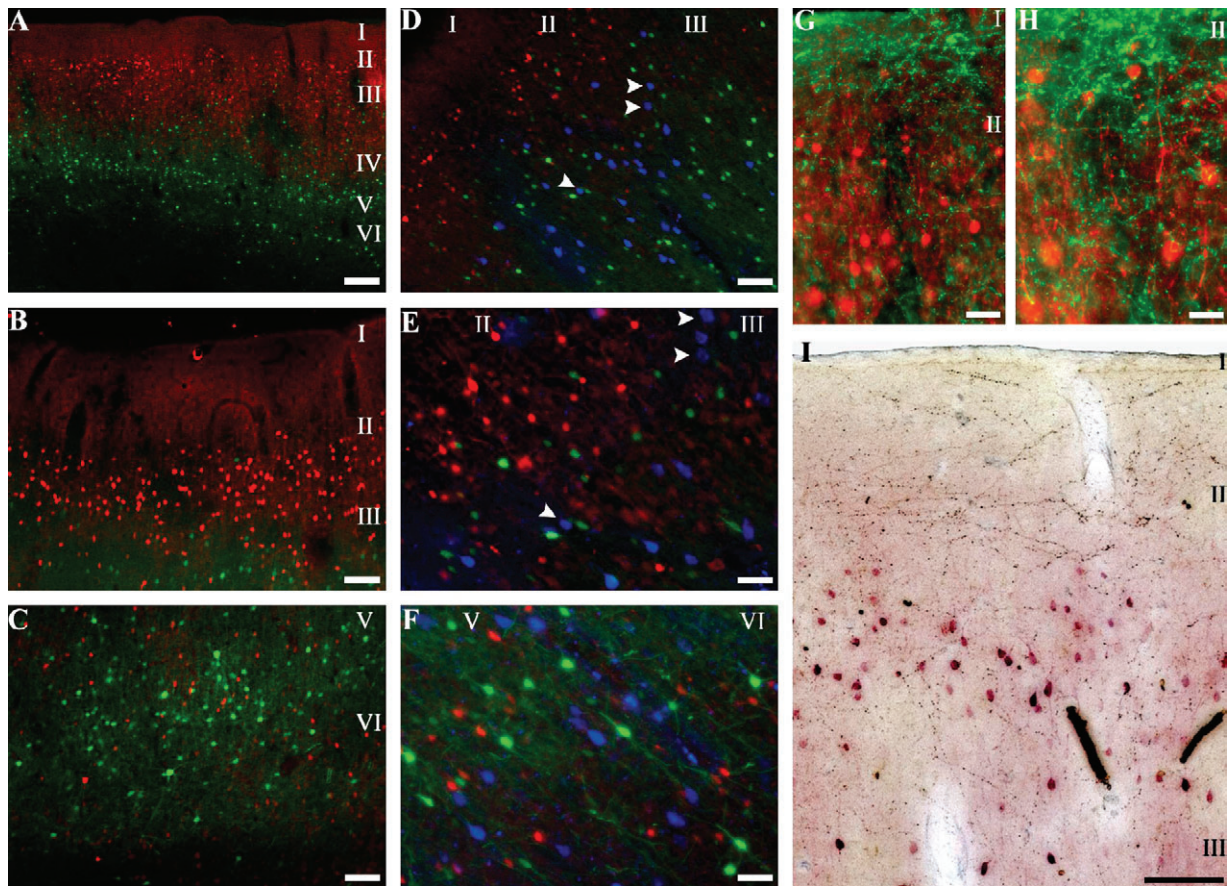


Figure 1. The distribution of CB+ and PV+ neurons and their relationship to prefrontal connections in superior temporal cortices. (A) Photomicrograph of coronal section in tissue treated for immunofluorescence, showing CB+ neurons (red) found most densely in the superficial layers of superior temporal cortex. PV+ neurons (green) were densest in the middle-deep layers. (B) CB+ and (C) PV+ neurons at higher magnification. The example is from area Ts2 in case BF. (D) Projection neurons (blue) in the upper layers of superior temporal area Ts1 directed to prefrontal area 9 (case BHb) and their relationship to local CB+ (red) and PV+ (green) neurons; (E) Section from D shown at higher magnification. (F) Projection neurons (blue) directed to prefrontal area 9 were intermingled mostly with PV neurons (green) in the deep layers and in layer III of superior temporal area Ts1 (case BHb). (G) BDA-labeled axonal fibers (green) from prefrontal area 10 (case BC) terminated heavily in layer I and II of superior temporal area Ts2 among CB+ neurons (red). Composite image in G was prepared in Photoshop by superimposing the same area from two serial sections, one processed for BDA, with label converted to green pseudocolor, and a second section processed for fluorescence microscopy showing CB+ neurons in red, as described in Materials and Methods; (H) Section from G shown at higher magnification. (I) BDA-labeled axonal fibers (brown) from prefrontal area 10 (case BC) terminated heavily in layer I and layer II, among CB positive neurons (purple) in superior temporal area Ts2, in tissue treated for double immunocytochemistry for brightfield microscopy. Scale bars: A = 250 μ m; B, C, D, I = 100 μ m; E, F, G = 50 μ m; H = 25 μ m.

Serial reconstruction of injection sites showed that injections encompassed all cortical layers and the needle tracts were restricted to the cortical mantle. In one case the tracer was applied to a small piece of gelfoam and placed on the pial surface, and the injection site was restricted to the superficial layers as intended (case BHb).

Topography and Laminar Terminations of Axons from Prefrontal Areas in Auditory Association Areas

For anterograde analysis we focused on the pattern of termination of area 10 and area 32, which have robust connections (Barbas and Mesulam, 1985; Barbas *et al.*, 1999), and a demonstrated and specific influence on superior temporal cortices at the functional level (Jürgens and Müller-Preuss, 1977; Müller-Preuss *et al.*, 1980; Müller-Preuss and Ploog, 1981; Heffner and Heffner, 1986). Quantitative analysis of bouton terminations was limited to the superior temporal gyrus and adjacent parts of the superficial part of the superior temporal sulcus, and dorsal and dorsomedial temporal pole. Labeled boutons were seen in other areas, including prefrontal and cingulate areas, but these were not analyzed for this study.

Anterograde data were obtained from six rhesus monkeys. The injection sites in areas 10, 32 and 11 are shown in Figure 6. In five cases the tracer was BDA, and in two of these the injection was in a small part of area 32 (cases AY, BG), and in three in area 10, including its rostral (case BA), or caudal parts (cases BC, BF). In one of the latter cases, the injection included a small part of adjacent area 9 (case BC). In the only case with HRP-WGA and analysis of anterograde label, the injection was in a small part of area 11 (Fig. 6, case AM).

Labeled boutons from area 32 terminated mostly in areas Ts1 and Ts2 (Fig. 7C, case AY; Fig. 8B,D), as well as in the dorso-medial and dorsolateral parts of the temporal pole (Fig. 8F). Only a few boutons were noted in parainsular area pal, or area Ts3 (not shown). In cases with injection in the caudal part of dorsal area 10, most labeled boutons were found more caudally within auditory association area Ts3 (Fig. 9), followed by areas Ts1 and Ts2 (Fig. 7A,B, cases BC, BF; Fig. 8A,C). In contrast, a rostral and ventral part of area 10 issued sparse projections to area Ts3, but issued moderate to robust projections to areas Ts2 and Ts1 (Fig. 7D, case BA). In all cases with injection in area 10 we also saw a few but consistent terminations in dorsal

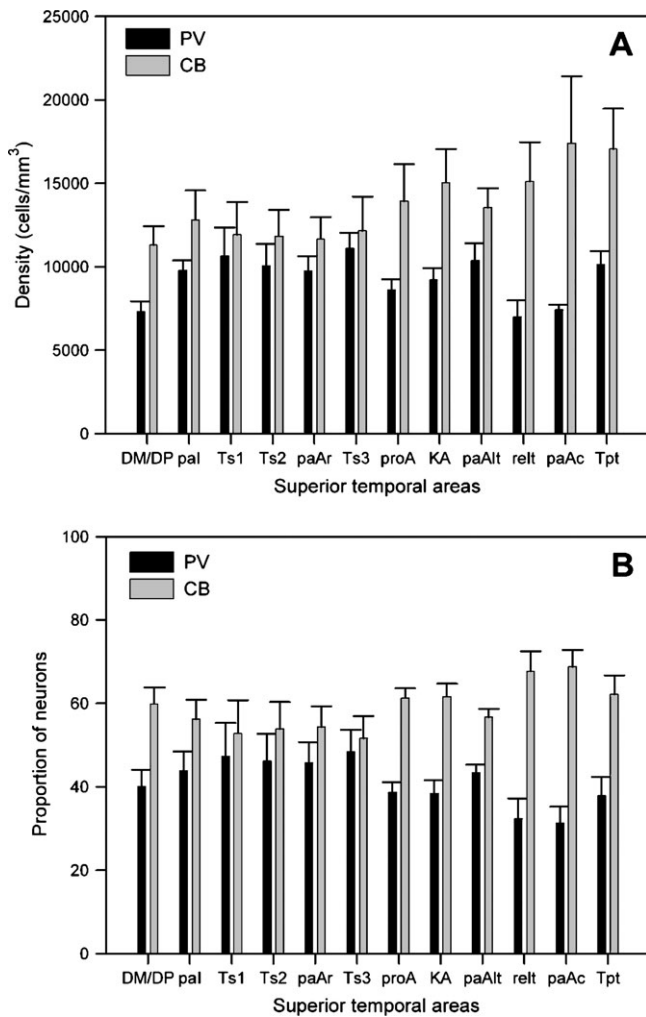


Figure 2. Distribution of parvalbumin (PV) and calbindin (CB) positive neurons in superior temporal areas. (A) Density of PV (black bars) and CB neurons (gray bars). (B) Proportion of CB (gray bars) and PV (black bars) neurons in superior temporal cortices. Data were analyzed using stereological procedures.

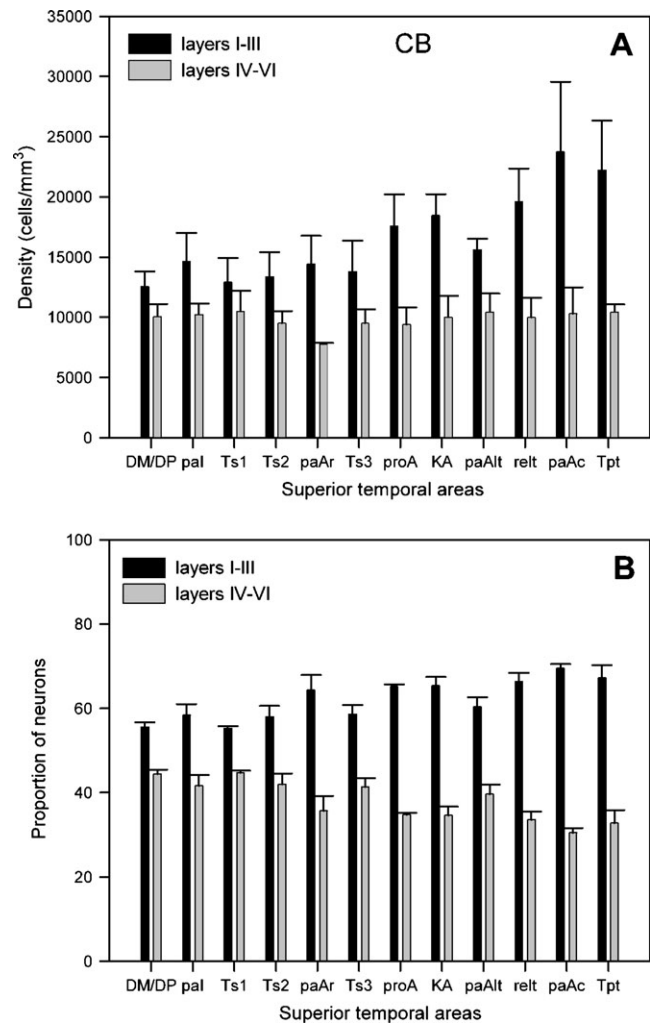


Figure 3. Laminar distribution of calbindin positive neurons in superior temporal cortices. (A) Laminar density distribution; (B) normalized laminar density.

temporal polar cortex, including its dorsomedial (DM Pole) and dorsolateral (DP) components (Fig. 7A,D; cases BC, BA; Fig. 8E). In addition, light projections from the caudal part of area 10 terminated in posterior high-order auditory association area paAlt as well (Fig. 9; cases BC, BF).

We also obtained quantitative data on the density of anterograde label in a case with injection of HRP-WGA in orbitofrontal area 11 using optical density analysis, as described previously (Rempel-Clower and Barbas, 2000). The highest density of anterograde label was found in the dorsal temporal polar region (37% of total label), and in area Ts1 (36% of total). Anterograde label was also found in area Ts2 (20%), and to a lesser extent in area Ts3 (7%).

In cases with a significant number of boutons in the temporal pole (>50), most were found in the deep layers (IV-VI; Fig. 8E,F), as shown for the three cases with injection in area 10 (Fig. 10). The same pattern was seen for cases with injection in area 32 (not shown). In contrast, in areas Ts1-Ts3 and paAlt, the majority (70-90%) of boutons were found in the upper layers (I-III), and the rest were distributed in the middle and deep layers (layers IV-VI; Fig. 10). The upper layers were most

prominently innervated by area 10, particularly in posterior auditory association area paAlt (93%, case BC), and to a lesser extent in areas Ts1-Ts3 (79-87%; cases BC, BF). However, the distribution of boutons in the upper layers was comparatively less pronounced for a rostral area 10 site (area Ts1 = 71%; area Ts2 = 69%; case BA), and for area 32 (area Ts1 = 77%; Ts2 = 68%; case BG; not shown).

We saw a similar pattern of terminations from orbitofrontal area 11 (not shown). In the dorsal temporal pole, label was found in the deep layers (51% of the total in this area), and in the upper layers (49%). Similarly, in area Ts1 label assumed a columnar distribution (layers I-III = 47%; layers IV-VI = 53%). In contrast, in area Ts2 terminations in the upper layers predominated (88%), and in area Ts3 a much lighter density of anterograde label was found exclusively in the upper layers.

Origin of Projection Neurons in Superior Temporal Association Areas Directed to Prefrontal Areas

As shown in Figure 6, data were obtained from nine animals with injections of retrograde tracers in dorsomedial (area 32, case AE; medial area 9, case AO; area 9/10, case BHB), and orbitofrontal areas (area OPro, cases AF, ALy, area OPro/OPAll,

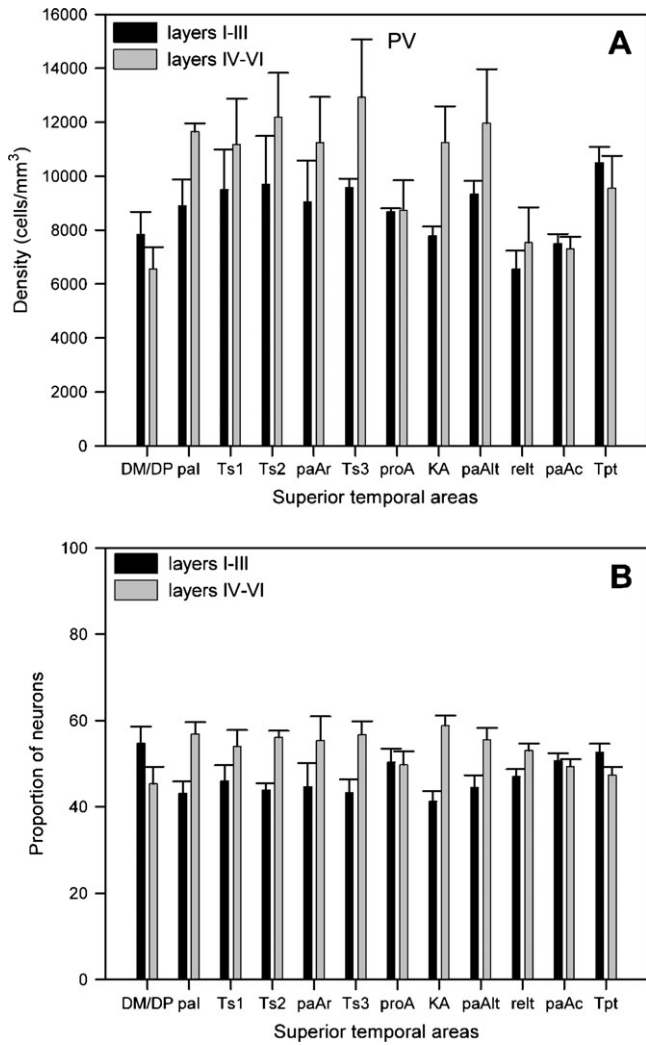


Figure 4. Laminar distribution of parvalbumin-positive neurons in superior temporal cortices. (A) Laminar density distribution; (B) normalized laminar density.

case AG; area 13, case AJb; area O12, case BAB; area 11, case AM). We also obtained qualitative data on the origin of projection neurons in superior temporal areas in cases with BDA injections (described above), but these were not used for quantitative analysis since the BDA used was optimal for anterograde but not retrograde labeling. Nevertheless, the topography of projection neurons was the same as for anterograde label described above (Fig. 8C,F).

Projection neurons from all prefrontal sites were distributed in the same sites that included anterograde label, including areas Ts1-Ts3, dorsomedial and dorsolateral temporal pole, and to a lesser extent in areas paI, proA and paAlt. The normalized laminar distribution of projection neurons in all areas and for all cases is shown in Figure 11. In the dorsal and dorsomedial temporal pole and in area paI most projection neurons originated in the deep layers (V-VI). In contrast, projection neurons in all other areas were most prevalent in the supragranular layers (II-III), though in areas Ts1 and Ts2 they were comparable in the supragranular and deep layers (Fig. 11). The supragranular predominance was most striking in posterior auditory association areas Ts3 and paAlt.

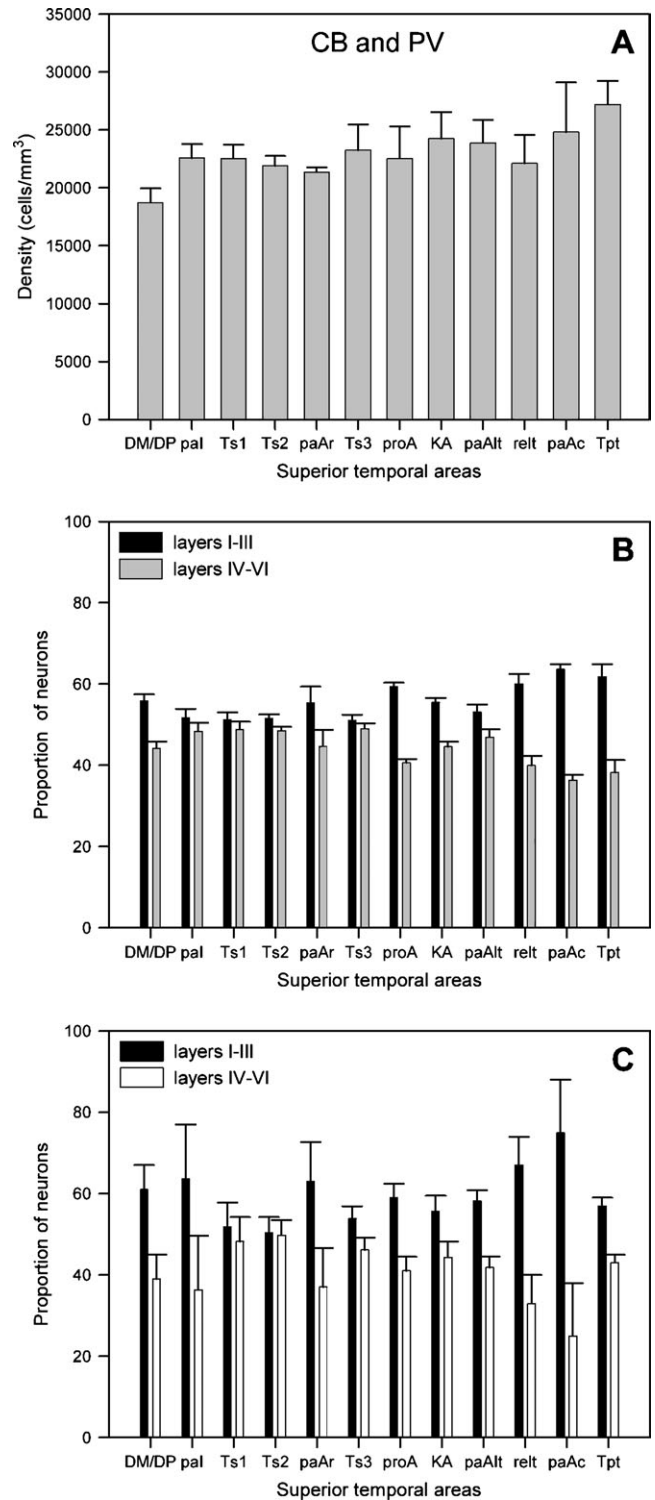


Figure 5. Combined density of PV and CB neurons in layers I-III and IV-VI of superior temporal cortices using two methods. (A) Combined density of PV and CB using 3D stereological procedure. (B) The same data as in A, showing the normalized laminar distribution of CB and PV neurons. (C) Normalized laminar density of PV and CB neurons obtained from tissue treated for immunofluorescence, as estimated in two dimensions. The two methods yielded comparable results.

Relationship of Connections to the Overall Distribution of CB+ and PV+ Neurons in Superior Temporal Areas

We then compared the laminar distribution of connections for areas with significant label (>20 neurons or >50 boutons) with

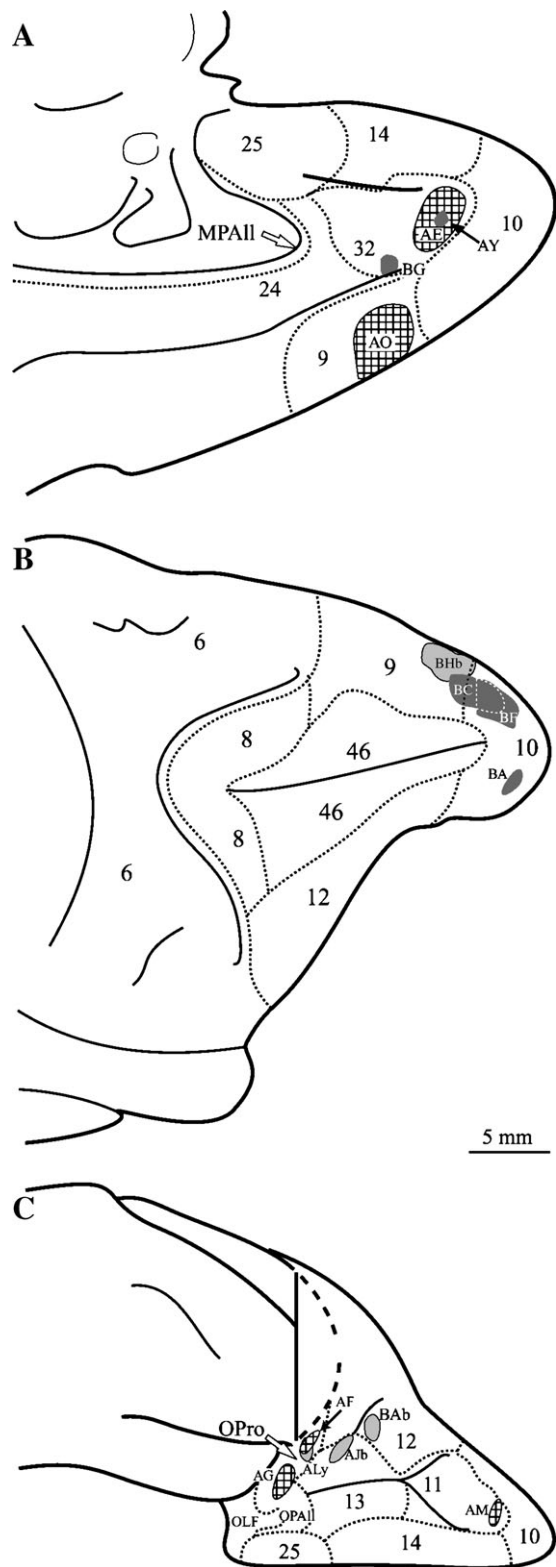


Figure 6. Injection sites in prefrontal cortices. (A) Medial surface; (B) lateral surface; (C) basal surface. Dark gray, BDA tracer; light gray, fluorescent tracers: b, fast blue; y, diamidino yellow; checkered pattern, HRP-WGA.

the combined density distribution of CB+ and PV+ neurons (Fig. 12A), shown also separately for each neurochemically identified interneuron class (Fig. 12B). In areas Ts1–Ts3, the relative laminar distribution of projection neurons paralleled the overall

distribution of CB+ and PV+ neurons. In contrast, in the dorsomedial and dorsal temporal pole (DM/DP) most projection neurons were found in the deep layers (V–VI), whereas the complement of CB+ and PV+ neurons was denser in the upper layers (Fig. 12). The same pattern was seen in the adjacent area paI (not shown). Moreover, the same lopsided relationship was noted for the termination of axonal boutons, which were most densely distributed in the deep layers of dorsal and dorsomedial temporal polar cortices. In contrast, in other temporal areas the great majority of boutons terminated in layers I, II and the upper part of layer III (Fig. 12).

Discussion

Superior Temporal Areas Have Distinct Profiles of Two Neurochemical Classes of Inhibitory Neurons

The functional linkage of prefrontal and superior temporal cortices is an excellent demonstration of the role of prefrontal areas in selecting relevant signals and ignoring irrelevant signals in behavior (Chao and Knight, 1997). The prefrontal cortex exercises this influence within a microenvironment that varies by area and layer with respect to distinct classes of inhibitory interneurons labeled with CB or PV. In the superior temporal region CB+ neurons were most prevalent in a band in the superficial layers, particularly layer II, while PV+ neurons were most densely distributed in a central band at the bottom of layer III to upper layer V, consistent with the complementary laminar distribution of these neurochemically identified classes of interneurons in the cortex (Hendry *et al.*, 1989; DeFelipe *et al.*, 1989a, 1990; Condé *et al.*, 1994; Gabbott and Bacon, 1996; reviewed in Hof *et al.*, 1999).

Calbindin-positive neurons outnumbered the PV in all superior temporal areas, but to a different extent. The two populations were comparable in areas Ts1–Ts3. However, CB+ neurons outnumbered the parvalbumin in the primary auditory area (area KA or A1) and posterior high-order association areas, due to their higher density in the upper layers. In contrast, regional differences in PV+ neurons reflected differences in their distribution in the deep layers. The complement of CB+ and PV+ neurons was lowest in the temporal pole, and highest in posterior high-order association area Tpt.

Comparison with Previous Studies

In another macaque species (*M. fascicularis*) an estimate for CB+ neurons was considerably lower for the primary auditory cortex, and PV+ was somewhat lower than, though comparable to, the present findings (Glezer *et al.*, 1998). The discrepancies may be attributed to differences in species, the antibody used and the quantitative approaches used in the two studies. Calbindin labels non-pyramidal as well as some pyramidal neurons, though the latter are comparatively few and lightly labeled (DeFelipe *et al.*, 1989a, 1990; for review see Hof *et al.*, 1999). Labeling of pyramidal neurons by CB depends largely on the antibody used, and can range from a negligible number to a substantial proportion of labeled neurons (Gonzalez-Albo *et al.*, 2001). The antibody we used does not appear to label a significant number of pyramidal neurons (Gonzalez-Albo *et al.*, 2001), and CB+ pyramidal neurons were sparse in our material. This evidence suggests that CB labeled primarily inhibitory neurons in this study.

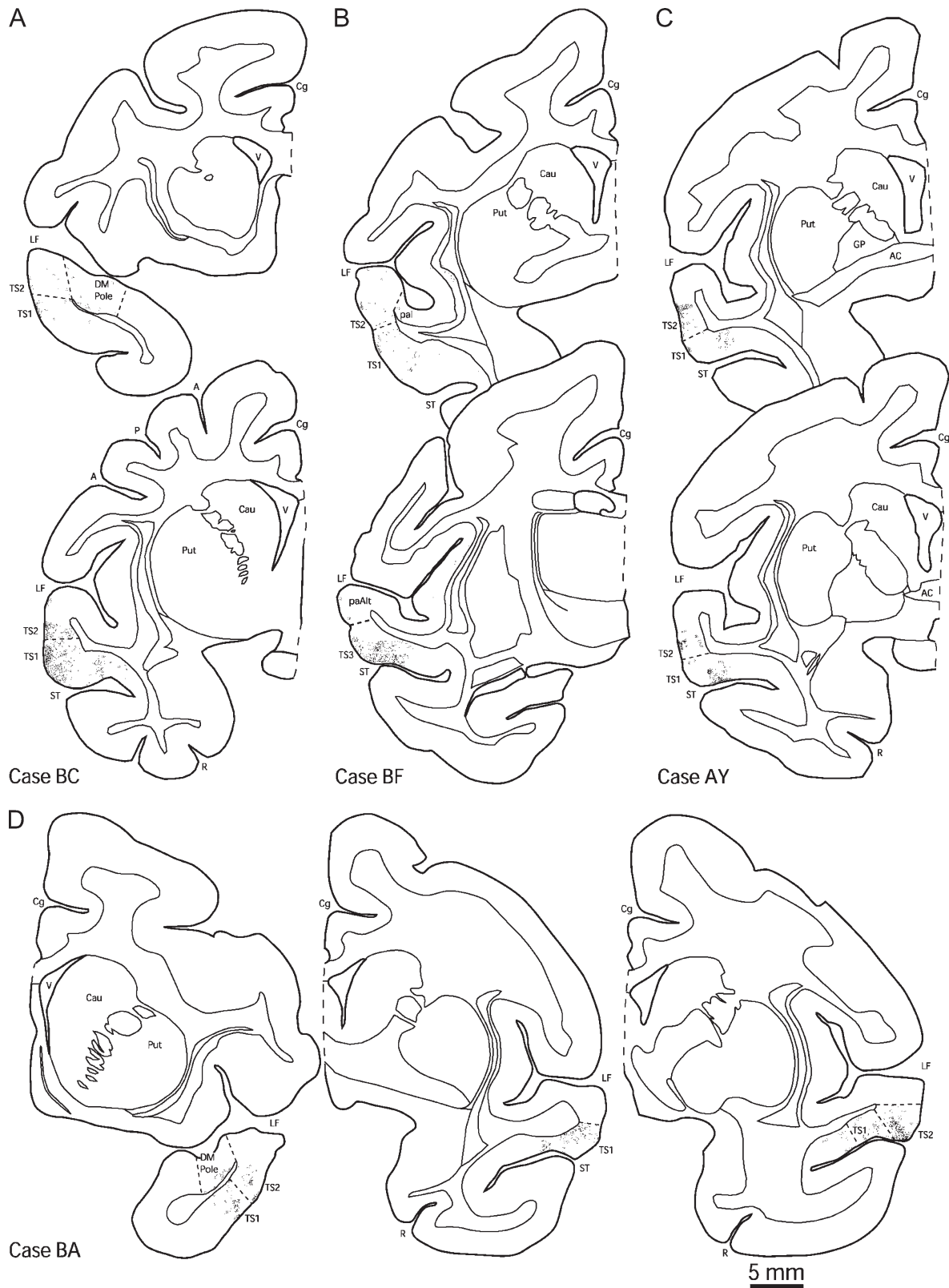


Figure 7. Prefrontal axonal terminations in superior temporal cortices after injection of BDA in prefrontal cortices, shown in coronal sections. (A) Injection of tracer was in area 10 (case BC). (B) Injection of tracer was in area 10 (lateral, caudal part, case BF). (C) Injection of tracer was in area 32 in the anterior cingulate (case AY). (D) Injection of tracer was in the rostral part of area 10 (case BA). For cases BC, BF and AY, medial is to the right, and rostral sections are on top. For case BA, medial is to the left and rostral sections are on the left.

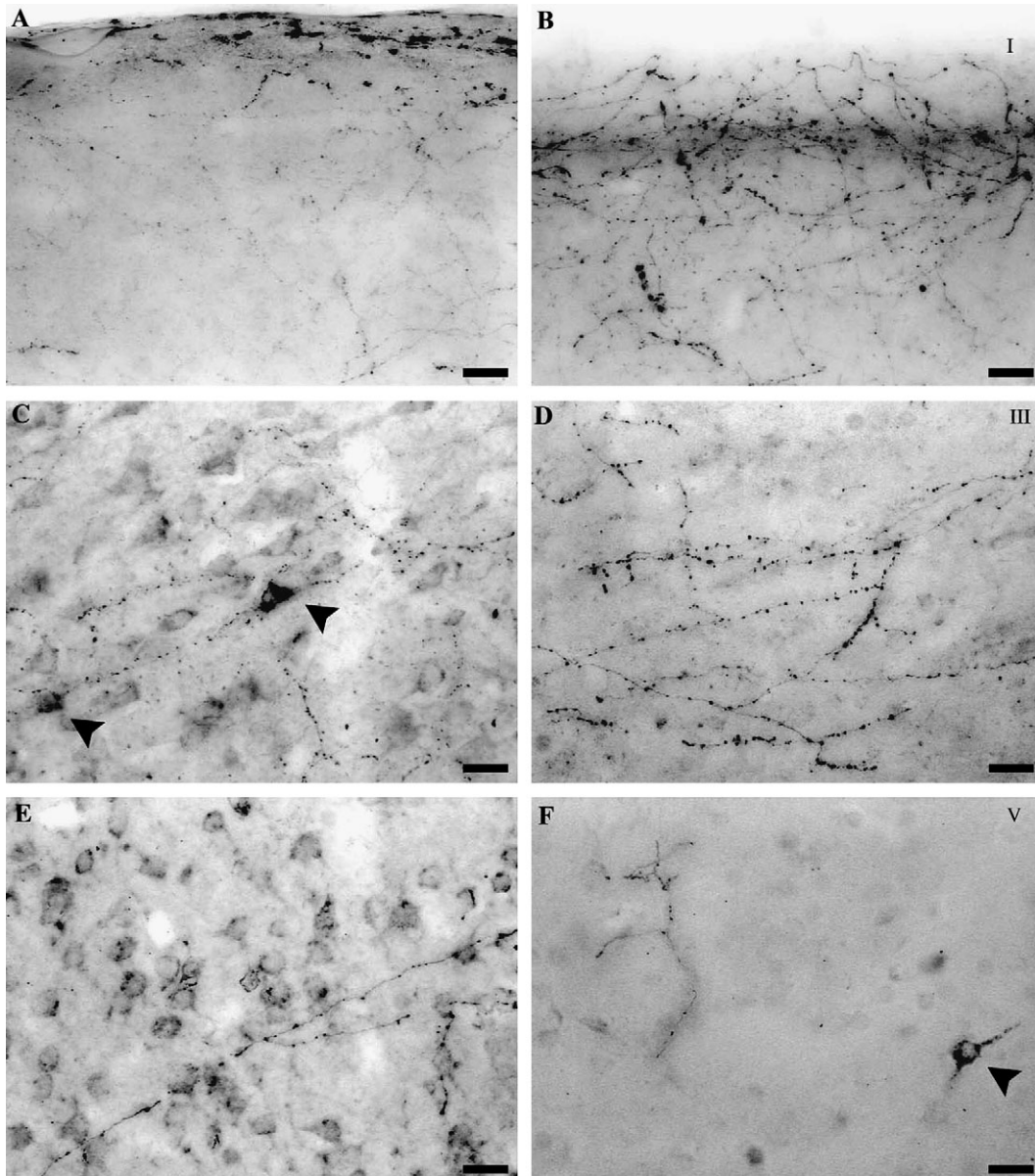


Figure 8. Photomicrographs showing BDA-labeled prefrontal axons and boutons terminating in superior temporal cortices. (A, C, E) Axonal terminations in a case with injection of BDA in lateral area 10 (case BC). (B, D, F) Axonal terminations in a case with injection of BDA in medial area 32. (A, B) Terminations in the upper layers (I to upper layer III) of superior temporal area Ts2. (C, D) Terminations in layer III in superior temporal area Ts2. (E, F) Terminations in deep layers V–VI in the dorsal part of the temporal pole. Arrowheads show sporadic labeled projection neurons. Scale bar = 25 μ m.

Previous studies, using different antibodies, have shown that the density of CB+ neurons increased in a direction from caudal to rostral ventral visual and auditory association areas, a finding attributed to the higher prevalence of CB+ pyramidal neurons in progressively rostral temporal areas (Kondo *et al.*, 1994, 1999). When pyramidal CB+ neurons were discounted, the density of non-pyramidal CB+ neurons was comparable among the rostral and intermediate superior temporal cortices (Kondo *et al.*, 1999). The distribution and numbers of CB+ neurons in these superior temporal areas (areas Ts1–Ts3) were also comparable in our study, suggesting that CB+ pyramidal neurons were not a significant factor in our results. However, in the considerably larger sample of areas examined here, we noted consistent

differences in CB+ neurons among superior temporal areas, with higher densities in posterior superior temporal association areas.

Laminar Pattern of Prefrontal Connections in Superior Temporal Areas

The anterior lateral, medial and orbitofrontal areas investigated were most densely connected with the rostral half of the superior temporal cortex (the temporal pole and areas Ts1–Ts3), and to a lesser extent with areas proA, paI and paAlt, consistent with previous findings (Jacobson and Trojanowski, 1977; Müller-Preuss *et al.*, 1980; Barbas and Mesulam, 1981, 1985; Vogt and Pandya, 1987; Petrides and Pandya, 1988; Barbas,

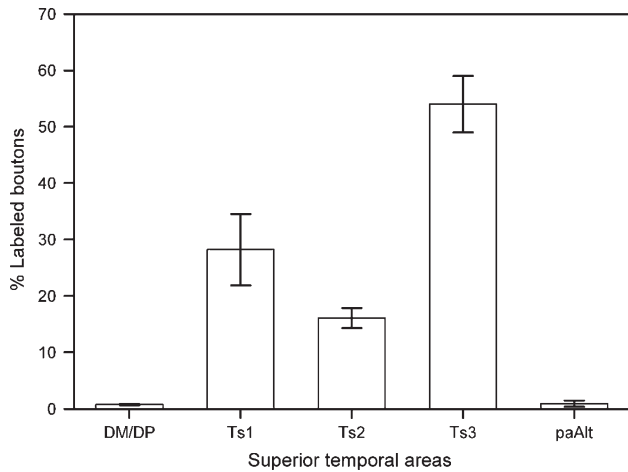


Figure 9. Normalized distribution of BDA labeled boutons in superior temporal areas in two cases with injection of BDA in the caudal part of dorsal area 10 (cases BF, BC).

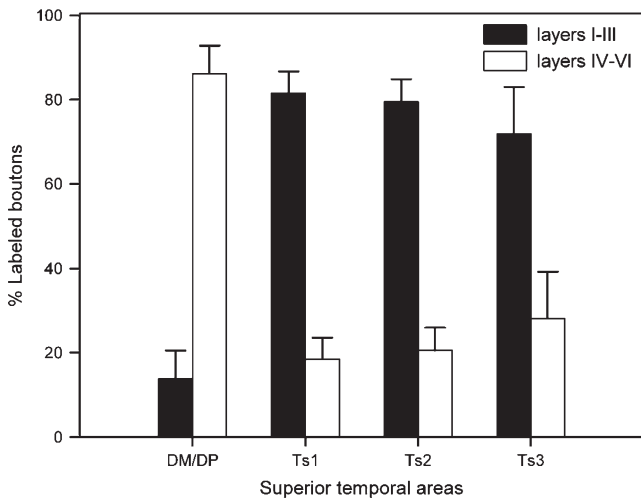


Figure 10. Normalized laminar density of labeled boutons in superior temporal areas in three cases with injection of BDA in prefrontal area 10. Most labeled boutons in the temporal pole were found in the deep layers, whereas in all other superior temporal cortices most were found in the superficial layers (I-III).

1988; Romanski *et al.*, 1999a; Kondo *et al.*, 2003). Axons from prefrontal areas 10 and 32 terminated overwhelmingly in the upper layers (I-III), and especially in layer I of areas Ts1-Ts3. In marked contrast, axons from areas 10 and 32 terminated primarily in the deep layers of superior temporal polar areas.

In most superior temporal cortices projection neurons directed to prefrontal areas were found in layers II-III and to a lesser extent in layers V-VI. The supragranular predominance was accentuated for posterior area Ts3 and area paAlt. In contrast, projection neurons in the temporal pole were found mostly in the deep layers. The above anterograde and retrograde patterns are consistent with reciprocity rules of connections linking other cortical areas, which generally originate and terminate in different layers for any set of interconnected areas (reviewed in Felleman and Van Essen, 1991). Moreover, the graded laminar pattern of connections supports the structural model, which states that the relative distribution of connections in cortical layers is dependent on the structural rela-

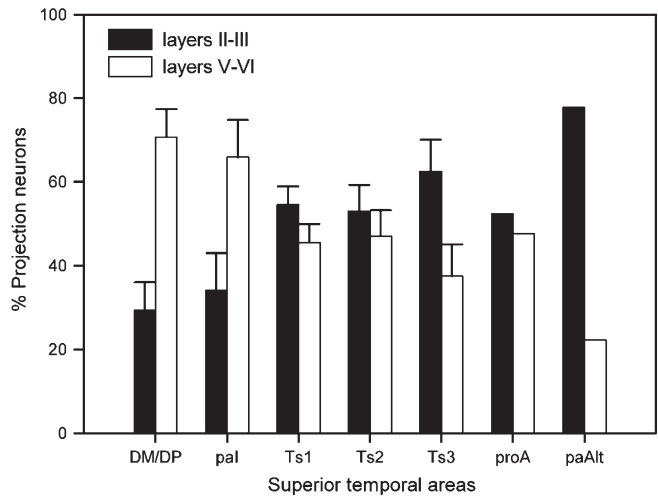


Figure 11. Normalized laminar density of projection neurons in superior temporal areas directed to anterior lateral, medial and orbitofrontal cortices. The laminar distribution of projection neurons in superior temporal areas was graded: projection neurons in anterior superior temporal polar (DM/DP) and the adjacent parainsular area (area pal) were found mostly in the deep layers, and in progressively more caudal superior temporal areas the distribution of projection neurons shifted progressively to the superficial layers (II-III).

tionship of the connected areas, which is also graded (Barbas and Rempel-Clower, 1997; Rempel-Clower and Barbas, 2000).

Relationship of Prefrontal Connections to Inhibitory Interneurons in Superior Temporal Areas

Projection Neurons Directed to Prefrontal Areas Overlapped Extensively with PV+ Neurons in the Middle Cortical Layers of Superior Temporal Areas

When the prefrontal connections and local inhibitory neuronal profiles were compared in superior temporal areas several key relationships emerged, as summarized in Figure 12. In areas Ts1-Ts3 the relative distribution of the combined inhibitory neurons closely matched the laminar distribution of projection neurons directed to prefrontal areas. Projection neurons in the deep part of layer III, in particular, and in layer V, were highly intermingled with PV+ neurons (Fig. 1D-F). The latter mark a neurochemical group of inhibitory interneurons that innervate dendritic and axonal sites close to the cell body of other neurons (DeFelipe *et al.*, 1989b; Kawaguchi and Kubota, 1997). The middle layers of the cortex, where PV+ neurons predominate, are also the targets of 'forward' projections from earlier processing sensory areas. There is evidence that stimulation of visual 'forward' pathways leads to monosynaptic excitation followed by disynaptic inhibition at the site of termination (Shao and Burkhalter, 1999). By analogy with the visual system, there may be a similar pattern of response with stimulation of distinct auditory-related pathways. Forward pathways in sensory systems transmit feature-specific signals to higher-order areas, terminating in the middle layers, including the lower part of layer III. Neurons in layer III make up the overwhelming majority of projection neurons directed to prefrontal cortices, as shown here and in previous studies (for review and earlier literature see Barbas, 2000). The close relationship of PV interneurons to projection neurons may

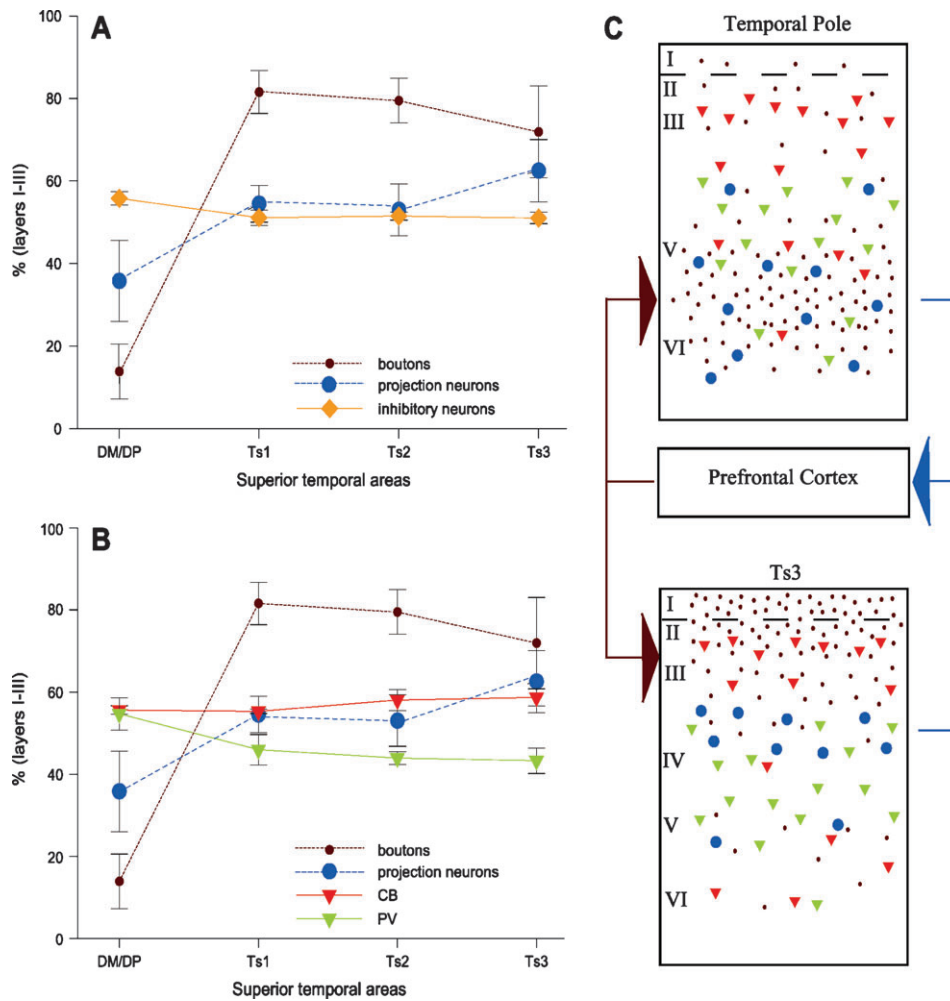


Figure 12. The relationship of connections to the distribution of inhibitory neurons labeled with PV and CB. (A) Relationship of connections to the combined density of CB and PV interneurons. (B) Relationship of connections to CB and PV depicted separately. (C) Sketch summarizing the predominant pattern of connections of prefrontal cortices with the agranular and dysgranular (limbic) parts of the temporal pole (top) and with a caudal eulaminate area of the superior temporal cortex (bottom), and their relationship to PV+ (green triangles) and CB+ (red triangles) inhibitory interneurons. Brown arrows (left) show the predominant laminar termination of prefrontal axons in superior temporal areas; blue arrow (right) shows the predominant laminar origin of projection neurons in superior temporal areas directed to prefrontal cortex.

help restrict the signals transmitted to the prefrontal cortex through lateral inhibition.

Axons from Prefrontal Cortices Overlapped Extensively with CB+ Neurons in the Upper Layers of Most Superior Temporal Areas

In sharp contrast to projection neurons, axons originating from prefrontal areas terminated overwhelmingly in the upper layers of superior temporal areas, avoiding the middle layers. Specifically, dense axonal terminations targeted layer I, followed by layer II and the upper part of layer III, at sites where CB+ neurons predominated. Calbindin is expressed in inhibitory double bouquet cells in the cortex, which innervate sites near the distal dendrites of other neurons (e.g. DeFelipe *et al.*, 1989a; Peters and Sethares, 1997). There is evidence that stimulation of 'feedback' pathways that terminate in layer I results in predominantly excitatory effects (Sandell and Schiller, 1982; Shao and Burkhalter, 1999). Based on evidence that long-distance pathways in the cortex are overwhelmingly excitatory (White and Keller 1989), projections from prefrontal cortices probably excite the apical dendrites of pyramidal neurons from deeper

layers, which may include projection neurons directed back to the same prefrontal areas. Such a bidirectional pathway may enable prefrontal areas to modulate the excitability of projection neurons and select feature specific information within the auditory modality. Activity in CB interneurons is important in the process of focusing on relevant features and suppressing distractors, according to a theoretical model based on neuronal responses during a working memory task in lateral prefrontal cortex (Wang *et al.*, 2004). Feedback projections, in general, terminate in long horizontal ribbons in cortical layer I, a circuit architecture that is ideal for eliminating distractors through interaction with CB+ neurons in adjacent layer II. The predominant terminations of prefrontal pathways in layers I-II may thus have an important role in masking distractors in auditory association cortices, which are enriched with CB+ neurons.

Feedback projections from lateral prefrontal cortices may influence task related activity of neurons in temporal cortices thought to have a role in attending to the task at hand (for reviews see Ullman, 1995; Payne *et al.*, 1996; Desimone, 1996; Lamme *et al.*, 1998; Bar, 2003). Prefrontal area 10 is specifically recruited when juggling multiple tasks in working memory,

such as keeping track of a main goal while attending to secondary tasks (Koechlin *et al.*, 1999). The strong projections from prefrontal area 10 to auditory association areas may have a distinct role in complex working memory tasks within the auditory domain, selecting relevant signals from a wide spectrum of auditory association areas with which it has bidirectional ties (Barbas and Mesulam, 1985; Barbas *et al.*, 1999; for review see Barbas *et al.*, 2002).

Medial prefrontal areas also showed robust feedback projections to the same superior temporal areas. Medial areas may have a role in emotional aspects of communication (for review see Vogt and Barbas, 1988; Barbas *et al.*, 2002), based on their robust projections to hypothalamic and brainstem autonomic structures associated with the expression of emotions (Rempel-Clower and Barbas, 1998; Barbas *et al.*, 2003).

Mismatch in Prevalence of Prefrontal Laminar Connections and Inhibitory Neurons in the Temporal Pole

The temporal pole stood apart among superior temporal areas as recipient of prefrontal projections that terminated in its middle and deep layers. Through such feedforward projections, prefrontal cortices may drive activity in temporal polar cortex, an area that is considered limbic by its dysgranular architecture and connections with other cortical and subcortical limbic structures (Gower, 1989; Kondo *et al.*, 2003). Temporal polar areas, in turn, issued feedback projections from their deep layers to prefrontal cortices, and may provide information on the emotional significance of auditory stimuli, including species-specific communication, recently associated with the temporal pole (Poremba *et al.*, 2004).

Like other superior temporal areas, the temporal pole showed the same relative laminar distribution of inhibitory neurons. A third class of neurochemically identified cortical interneurons positive for calretinin is also more prevalent in the superficial cortical layers in prefrontal and temporal cortices (del Rio and DeFelipe, 1997; DeFelipe *et al.*, 1999; Dombrowski *et al.*, 2001). These findings indicate that the relative laminar distributions of connections and local inhibitory neurons are mismatched in the temporal pole. As summarized in Figure 12C, the relationship of prefrontal connections to inhibitory interneurons thus differs in distinct superior temporal areas in a pattern that likely affects the functional dynamics in these pathways in behavior.

Implications for Neuropathology

The reduced efficacy of inhibitory control in auditory areas in patients with dorsolateral frontal lobe damage (Chao and Knight, 1997; Knight *et al.*, 1999) may be due to a disturbance of excitatory and inhibitory interactions in prefrontal-temporal pathways. Prefrontal cortical damage disrupts the process of filtering relevant signals and ignoring distractors (Gehring and Knight, 2002), perhaps through disconnection of robust prefrontal pathways that terminate among CB+ neurons in the upper layers of most superior temporal areas. Prefrontal damage may thus impair the ability to follow conversations in noisy environments.

The contrasting prevalence of prefrontal connections in the deep layers and inhibitory interneurons in the upper layers in the temporal pole differs markedly from the patterns seen in other superior temporal cortices (Fig. 12C). The laminar mismatch in the prevalence of connections and inhibitory neurons in the temporal pole resembles the pattern seen in other limbic cortices, within the posterior medial and posterior orbitofrontal

cortices (Dombrowski *et al.*, 2001). This evidence suggests that the dynamics of excitatory and inhibitory control are different in limbic cortices than in eulaminate areas. Moreover, PV+ neurons, which are prevalent in the deep cortical layers, become increasingly vulnerable in Alzheimer's disease as projection neurons degenerate (Arai *et al.*, 1987; Solodkin *et al.*, 1996). The preferential degeneration of neurons in the deep layers of several limbic cortices suggests that they become disconnected from bidirectional pathways that link them with prefrontal cortices.

Abbreviations

A1	auditory area 1 (primary auditory)
AC	anterior commissure
AL	anterior lateral auditory belt
Cau	caudate
Cg	cingulate sulcus
CL	caudal lateral auditory belt
CP	caudal auditory parabelt
CM	caudomedial auditory belt
DM/DP	dorsomedial/dorsal temporal pole
GP	globus pallidus
KA	koniocortex (primary auditory)
LF	lateral fissure
M	medial area (surrounding primary auditory)
MPAll	medial periallocortex (dysgranular cortex)
OLF	olfactory area
paAc	caudal parakoniocortex
paAlt	lateral parakoniocortex
paAr	rostral parakoniocortex
pal	parinsular
pro	proisocortex
proA	prokoniocortex
Put	putamen
R	rostral area (primary auditory)
relt	retroinsular-temporal
RM	rostromedial region
RP	rostral auditory parabelt
RT	rostrotemporal region
RTL	lateral rostrotemporal auditory belt
RTM	medial rostrotemporal auditory belt
ST	superior temporal sulcus
TG	temporal gyrus
TPa-p	agranular temporal pole
TPdg	dysgranular temporal pole
TPpAll	periallocortical temporal pole
TPproD	dorsal proisocortical temporal pole
Tpt	temperoparietal
Ts1	superior temporal area 1
Ts2	superior temporal area 2
Ts3	superior temporal area 3
V	ventricle

Notes

This work was supported by NIH grants from NINDS and NIMH.

Address correspondence to Helen Barbas, Boston University, 635 Commonwealth Avenue, Room 431, Boston, MA 02215, USA. Email: barbas@bu.edu.

References

- Arai H, Emson PC, Mountjoy CQ, Carassco LH, Heizmann CW (1987) Loss of parvalbumin-immunoreactive neurones from cortex in Alzheimer-type dementia. *Brain Res* 418:164-169.

- Bar M (2003) A cortical mechanism for triggering top-down facilitation in visual object recognition. *J Cogn Neurosci* 15:600-609.
- Barbas H (1988) Anatomic organization of basoventral and mediodorsal visual recipient prefrontal regions in the rhesus monkey. *J Comp Neurol* 276:313-342.
- Barbas H (1992) Architecture and cortical connections of the prefrontal cortex in the rhesus monkey. In: *Advances in neurology*, Vol. 57 (Chauvel P, Delgado-Escueta AV, Halgren E, Bancaud J, eds), pp. 91-115. New York: Raven Press.
- Barbas H (1993) Organization of cortical afferent input to orbitofrontal areas in the rhesus monkey. *Neuroscience* 56:841-864.
- Barbas H (2000) Complementary role of prefrontal cortical regions in cognition, memory and emotion in primates. *Adv Neurol* 84:87-110.
- Barbas H, Mesulam MM (1981) Organization of afferent input to subdivisions of area 8 in the rhesus monkey. *J Comp Neurol* 200:407-431.
- Barbas H, Mesulam MM (1985) Cortical afferent input to the principal region of the rhesus monkey. *Neuroscience* 15:619-637.
- Barbas H, De Olmos J (1990) Projections from the amygdala to basoventral and mediodorsal prefrontal regions in the rhesus monkey. *J Comp Neurol* 301:1-23.
- Barbas H, Rempel-Clover N (1997) Cortical structure predicts the pattern of corticocortical connections. *Cereb Cortex* 7:635-646.
- Barbas H, Ghashghaei H, Dombrowski SM, Rempel-Clover NL (1999) Medial prefrontal cortices are unified by common connections with superior temporal cortices and distinguished by input from memory-related areas in the rhesus monkey. *J Comp Neurol* 410:343-367.
- Barbas H, Ghashghaei H, Rempel-Clover N, Xiao D (2002) Anatomic basis of functional specialization in prefrontal cortices in primates. In: *Handbook of neuropsychology* (Grafman J, ed.), pp. 1-27. Amsterdam: Elsevier.
- Barbas H, Saha S, Rempel-Clover N, Ghashghaei T (2003) Serial pathways from primate prefrontal cortex to autonomic areas may influence emotional expression. *BMC Neurosci* 4:25.
- Benes FM, Lange N (2001) Two-dimensional versus three-dimensional cell counting: a practical perspective. *Trends Neurosci* 24:11-17.
- Brodmann K (1909) Vergleichende Lokalisationslehre der Grosshirnrinde in ihren Prinzipien dargestellt auf Grund des Zellenbaues. Leipzig: Barth.
- Carmichael ST, Price JL (1995) Limbic connections of the orbital and medial prefrontal cortex in macaque monkeys. *J Comp Neurol* 363:615-641.
- Chao LL, Knight RT (1997) Prefrontal deficits in attention and inhibitory control with aging. *Cereb Cortex* 7:63-69.
- Chao LL, Knight RT (1998) Contribution of human prefrontal cortex to delay performance. *J Cogn Neurosci* 10:167-177.
- Chiry O, Tardif E, Magistretti PJ, Clarke S (2003) Patterns of calcium-binding proteins support parallel and hierarchical organization of human auditory areas. *Eur J Neurosci* 17:397-410.
- Condé F, Lund JS, Jacobowitz DM, Baimbridge KG, Lewis DA. (1994) Local circuit neurons immunoreactive for calretinin, calbindin D-28k or parvalbumin in monkey prefrontal cortex: distribution and morphology. *J Comp Neurol* 341:95-116.
- Cusick CG (1997) The superior temporal polysensory region in monkeys. In: *Cerebral cortex: extrastriate cortex in primates* (Rockland KS, Kaas JH, Peters A, eds), pp. 435-468. New York: Plenum Press.
- DeFelipe J, Hendry SH, Jones EG (1989a) Synapses of double bouquet cells in monkey cerebral cortex visualized by calbindin immunoreactivity. *Brain Res* 503:49-54.
- DeFelipe J, Hendry SH, Jones EG (1989b) Visualization of chandelier cell axons by parvalbumin immunoreactivity in monkey cerebral cortex. *Proc Natl Acad Sci USA* 86:2093-2097.
- DeFelipe J, Hendry SH, Hashikawa T, Molinari M, Jones EG (1990) A microcolumnar structure of monkey cerebral cortex revealed by immunocytochemical studies of double bouquet cell axons. *Neuroscience* 37:655-673.
- DeFelipe J, Gonzalez-Albo MC, del Rio MR, Elston GN (1999) Distribution and patterns of connectivity of interneurons containing calbindin, calretinin, and parvalbumin in visual areas of the occipital and temporal lobes of the macaque monkey. *J Comp Neurol* 412:515-526.
- del Rio MR, DeFelipe J (1997) Synaptic connections of calretinin-immunoreactive neurons in the human neocortex. *J Neurosci* 17:5143-5154.
- Dermon CR, Barbas H (1994) Contralateral thalamic projections predominantly reach transitional cortices in the rhesus monkey. *J Comp Neurol* 344:508-531.
- Desimone R (1996) Neural mechanisms for visual memory and their role in attention. *Proc Natl Acad Sci USA* 93:13494-13499.
- Dolan RJ, Fletcher P, Frith CD, Friston KJ, Frackowiak RSJ, Grasby PM (1995) Dopaminergic modulation of impaired cognitive activation in the anterior cingulate cortex in schizophrenia. *Nature* 378:180-182.
- Dombrowski SM, Hilgetag CC, Barbas H (2001) Quantitative architecture distinguishes prefrontal cortical systems in the rhesus monkey. *Cereb Cortex* 11:975-988.
- Elston GN, Gonzalez-Albo MC (2003) Parvalbumin-, calbindin-, and calretinin-immunoreactive neurons in the prefrontal cortex of the owl monkey (*Aotus trivirgatus*): a standardized quantitative comparison with sensory and motor areas. *Brain Behav Evol* 62:19-30.
- Felleman DJ, Van Essen DC (1991) Distributed hierarchical processing in the primate cerebral cortex. *Cereb Cortex* 1:1-47.
- Frith C, Dolan R (1996) The role of the prefrontal cortex in higher cognitive functions. *Brain Res Cogn Brain Res* 5:175-181.
- Fuster JM (1989) The prefrontal cortex. New York: Raven Press.
- Gabbott PL, Bacon SJ (1996) Local circuit neurons in the medial prefrontal cortex (areas 24a,b,c, 25 and 32) in the monkey: I. Cell morphology and morphometrics. *J Comp Neurol* 364:567-608.
- Galaburda AM, Pandya DN (1983) The intrinsic architectonic and connective organization of the superior temporal region of the rhesus monkey. *J Comp Neurol* 221:169-184.
- Gehring WJ, Knight RT (2002) Lateral prefrontal damage affects processing selection but not attention switching. *Brain Res Cogn Brain Res* 13:267-279.
- Glezer II, Hof PR, Morgane PJ (1998) Comparative analysis of calcium-binding protein-immunoreactive neuronal populations in the auditory and visual systems of the bottlenose dolphin (*Tursiops truncatus*) and the macaque monkey (*Macaca fascicularis*). *J Chem Neuroanat* 15:203-37.
- Gonzalez-Albo MC, Elston GN, DeFelipe J (2001) The human temporal cortex: characterization of neurons expressing nitric oxide synthase, neuropeptides and calcium-binding proteins, and their glutamate receptor subunit profiles. *Cereb Cortex* 11:1170-1181.
- Gower EC (1989) Efferent projections from limbic cortex of the temporal pole to the magnocellular medial dorsal nucleus in the rhesus monkey. *J Comp Neurol* 280:343-358.
- Gundersen HJ, Jensen EB, Kieu K, Nielsen J (1999) The efficiency of systematic sampling in stereology — reconsidered. *J Microsc* 193:199-211.
- Hackett TA, Stepniewska I, Kaas JH (1998) Subdivisions of auditory cortex and ipsilateral cortical connections of the parabelt auditory cortex in macaque monkeys. *J Comp Neurol* 394:475-495.
- Hackett TA, Stepniewska I, Kaas JH (1999) Prefrontal connections of the parabelt auditory cortex in macaque monkeys. *Brain Res* 817:45-58.
- Heffner HE, Heffner RS (1986) Effect of unilateral and bilateral auditory cortex lesions on the discrimination of vocalizations by Japanese macaques. *J Neurophysiol* 56:683-701.
- Hendry SH, Jones EG, Emson PC, Lawson DEM, Heizmann CW, Streit P (1989) Two classes of cortical GABA neurons defined by differential calcium binding protein immunoreactivities. *Exp Brain Res* 76:467-472.
- Hof PR, Glezer II, Condé F, Flagg RA, Rubin MB, Nimchinsky EA, Vogt Weisenborn DM (1999) Cellular distribution of the calcium-binding proteins parvalbumin, calbindin, and calretinin in the neocortex of mammals: phylogenetic and developmental patterns. *J Chem Neuroanat* 16:77-116.
- Howard CV, Reed MG (1998) Unbiased stereology, three-dimensional measurement in microscopy. Oxford: BIOS.
- Jacobson S, Trojanowski JQ (1977) Prefrontal granular cortex of the rhesus monkey I. Intrahemispheric cortical afferents. *Brain Res* 132:209-233.

- Jones EG, Dell'Anna ME, Molinari M, Rausell E, Hashikawa T (1995) Subdivisions of macaque monkey auditory cortex revealed by calcium-binding protein immunoreactivity. *J Comp Neurol* 362:153-170.
- Jürgens U, Müller-Preuss P (1977) Convergent projections of different limbic vocalization areas in the squirrel monkey. *Exp Brain Res* 29:75-83.
- Kaas JH, Hackett TA (2000) Subdivisions of auditory cortex and processing streams in primates. *Proc Natl Acad Sci USA* 97:11793-11799.
- Kawaguchi Y, Kubota Y (1997) GABAergic cell subtypes and their synaptic connections in rat frontal cortex. *Cereb Cortex* 7:476-486.
- Knight RT, Staines WR, Swick D, Chao LL (1999) Prefrontal cortex regulates inhibition and excitation in distributed neural networks. *Acta Psychol (Amst)* 101:159-178.
- Koechlin E, Basso G, Pietrini P, Panzer S, Grafman J (1999) The role of the anterior prefrontal cortex in human cognition. *Nature* 399:148-151.
- Kondo H, Hashikawa T, Tanaka K, Jones EG (1994) Neurochemical gradient along the monkey occipito-temporal cortical pathway. *Neuroreport* 5:613-616.
- Kondo H, Tanaka K, Hashikawa T, Jones EG (1999) Neurochemical gradients along monkey sensory cortical pathways: calbindin-immunoreactive pyramidal neurons in layers II and III. *Eur J Neurosci* 11:4197-4203.
- Kondo H, Saleem KS, Price JL (2003) Differential connections of the temporal pole with the orbital and medial prefrontal networks in macaque monkeys. *J Comp Neurol* 465:499-523.
- Kosaki H, Hashikawa T, He J, Jones EG (1997) Tonotopic organization of auditory cortical fields delineated by parvalbumin immunoreactivity in macaque monkeys. *J Comp Neurol* 386:304-316.
- Kritzer MF, Cowey A, Somogyi P (1992) Patterns of inter- and intralaminar GABAergic connections distinguish striate (V1) and extrastriate (V2, V4) visual cortices and their functionally specialized subdivisions in the rhesus monkey. *J Neurosci* 12:4545-4564.
- Lamme VA, Super H, Spekreijse H (1998) Feedforward, horizontal, and feedback processing in the visual cortex. *Curr Opin Neurobiol* 8:529-535.
- Merzenich MM, Brugge JF (1973) Representation of the cochlear partition on the superior temporal plane of the macaque monkey. *Brain Res* 50:275-296.
- Mesulam M-M, Mufson EJ (1982) Insula of the old world monkey. I: Architectonics in the insulo-orbito-temporal component of the paralimbic brain. *J Comp Neurol* 212:1-22.
- Mikkonen M, Soininen H, Pitkanen A (1997) Distribution of parvalbumin-, calretinin-, and calbindin-D28k-immunoreactive neurons and fibers in the human entorhinal cortex. *J Comp Neurol* 388:64-88.
- Miller EK, Cohen JD (2001). An integrative theory of prefrontal cortex function. *Annu Rev Neurosci* 24:167-202.
- Molinari M, Dell'Anna ME, Rausell E, Leggio MG, Hashikawa T, Jones EG (1995) Auditory thalamocortical pathways defined in monkeys by calcium-binding protein immunoreactivity. *J Comp Neurol* 362:171-194.
- Morel A, Garraghty PE, Kaas JH (1993) Tonotopic organization, architectonic fields, and connections of auditory cortex in macaque monkeys. *J Comp Neurol* 335:437-459.
- Müller-Preuss P, Ploog D (1981) Inhibition of auditory cortical neurons during phonation. *Brain Res* 215:61-76.
- Müller-Preuss P, Newman JD, Jürgens U (1980) Anatomical and physiological evidence for a relationship between the cingulate vocalization area and the auditory cortex in the squirrel monkey. *Brain Res* 202:307-315.
- Pandya DN, Seltzer B, Barbas H (1988) Input-output organization of the primate cerebral cortex. In: *Comparative primate biology*, Vol. 4: Neurosciences (Steklis HD, Erwin J, eds), pp. 39-80. New York: Alan R. Liss.
- Payne BR, Lomber SG, Villa AE, Bullier J (1996) Reversible deactivation of cerebral network components. *Trends Neurosci* 19:535-542.
- Peters A, Sethares C (1997) The organization of double bouquet cells in monkey striate cortex. *J Neurocytol* 26:779-797.
- Petrides M, Pandya DN (1988) Association fiber pathways to the frontal cortex from the superior temporal region in the rhesus monkey. *J Comp Neurol* 273:52-66.
- Poremba A, Saunders RC, Crane AM, Cook M, Sokoloff L, Mishkin M (2003) Functional mapping of the primate auditory system. *Science* 299:568-572.
- Poremba A, Malloy M, Saunders RC, Carson RE, Herscovitch P, Mishkin M (2004) Species-specific calls evoke asymmetric activity in the monkey's temporal poles. *Nature* 427:448-451.
- Rempel-Clower NL, Barbas H (1998) Topographic organization of connections between the hypothalamus and prefrontal cortex in the rhesus monkey. *J Comp Neurol* 398:393-419.
- Rempel-Clower NL, Barbas H (2000) The laminar pattern of connections between prefrontal and anterior temporal cortices in the rhesus monkey is related to cortical structure and function. *Cereb Cortex* 10:851-865.
- Roberts AC, Wallis JD (2000) Inhibitory control and affective processing in the prefrontal cortex: neuropsychological studies in the common marmoset. *Cereb Cortex* 10:252-262.
- Romanski LM, Bates JF, Goldman-Rakic PS (1999a) Auditory belt and parabelt projections to the prefrontal cortex in the rhesus monkey. *J Comp Neurol* 403:141-157.
- Romanski LM, Tian B, Fritz J, Mishkin M, Goldman-Rakic PS, Rauschecker JP (1999b) Dual streams of auditory afferents target multiple domains in the primate prefrontal cortex. *Nat Neurosci* 2:1131-1136.
- Sandell JH, Schiller PH (1982) Effect of cooling area 18 on striate cortex cells in the squirrel monkey. *J Neurophysiol* 48:38-48.
- Shao Z, Burkhalter A (1999) Role of GABAB receptor-mediated inhibition in reciprocal interareal pathways of rat visual cortex. *J Neurophysiol* 81:1014-1024.
- Shimamura AP (1995) Memory and frontal lobe function. In: *The cognitive neurosciences* (Gazzaniga MS, ed.), pp. 803-813. Cambridge, MA: MIT Press.
- Solodkin A, Veldhuizen SD, Van Hoesen GW (1996) Contingent vulnerability of entorhinal parvalbumin-containing neurons in Alzheimer's disease. *J Neurosci* 16:3311-3321.
- Suzuki WA, Amaral DG (1994) Perirhinal and parahippocampal cortices of the macaque monkey: cortical afferents. *J Comp Neurol* 350:497-533.
- Suzuki WA, Amaral DG (2003) Perirhinal and parahippocampal cortices of the macaque monkey: cytoarchitectonic and chemoarchitectonic organization. *J Comp Neurol* 463:67-91.
- Tian B, Reser D, Durham A, Kustov A, Rauschecker JP (2001) Functional specialization in rhesus monkey auditory cortex. *Science* 292:290-293.
- Ullman S (1995) Sequence seeking and counter streams: a computational model for bidirectional information in the visual cortex. *Cereb Cortex* 5:1-11.
- Vogt BA, Pandya DN (1987) Cingulate cortex of the rhesus monkey: II. Cortical afferents. *J Comp Neurol* 262:271-289.
- Vogt BA, Barbas H (1988) Structure and connections of the cingulate vocalization region in the rhesus monkey. In: *The physiological control of mammalian vocalization* (Newman JD, ed.), pp. 203-225. New York: Plenum.
- Von Bonin G, Bailey P (1947) *The neocortex of Macaca mulatta*. Urbana: The University of Illinois Press.
- Wang XJ, Tegner J, Constantinidis C, Goldman-Rakic PS (2004) Division of labor among distinct subtypes of inhibitory neurons in a cortical microcircuit of working memory. *Proc Natl Acad Sci USA* 101:1368-1373.
- West MJ, Gundersen HJG (1990) Unbiased stereological estimation of the number of neurons in the human hippocampus. *J Comp Neurol* 296:1-22.
- West MJ, Slomianka L, Gundersen HJG (1991) Unbiased stereological estimation of the total number of neurons in the subdivisions of the rat hippocampus using the optical fractionator. *Anat Rec* 231:482-497.
- White EL, Keller A (1989) *Cortical circuits synaptic organization of the cerebral cortex structure, function and theory*. Boston, MA and Basel: Birkhäuser.